OPEN ACCESS

1st International e-Conference on Energies
14 - 31 March 2014

http://sciforum.net/conference/ece-1

Conference Proceedings Paper - Energies „Whither Energy Conversion? Present Trends, Current Problems and Realistic Future Solutions”

Circuit Simulation for Solar Power Maximum Power Point Tracking with Different Buck-Boost Converter Topologies

Jaw-Kuen Shiau *, Min-Yi Lee , Yu-Chen Wei, and Bo-Chih Chen

Department of Aerospace Engineering, Tamkang University, Tamsui, New Taipei City, 25137, Taiwan; E-Mail:601430688@s01.tku.edu.tw (M.-Y. L.);601430662@s01.tku.edu.tw (Y.-C. W.); 601430670@s01.tku.edu.tw (B.-C. C.)

* Author to whom correspondence should be addressed; E-Mail: shiauj@mail.tku.edu.tw; Tel.: +886-2-2621-5656 ext. 3318; Fax: +886-2-2620-9746.

Received: 15 January 2014 / Accepted: 2 March 2014 / Published: 14 March 2014

Abstract: Power converter is one of the essential elements for effective utilization of renewable power sources. This paper focuses on the development of a circuit simulation model for solar power maximum power point tracking (MPPT) evaluation with different buck-boost power converter topologies including SEPIC, ZETA, and four-switch type buck-boost DC/DC converters. The circuit simulation model mainly includes three subsystems, namely, a PV emulator model, a buck-boost converter based MPPT system, and a fuzzy logic MPPT controller. A buck-boost converter based dual regulation (voltage regulation and current regulation) modes PV emulator is built to emulate the characteristics of the PV panel. The PV emulator is used to power the MPPT system. The MPPT system also contains a buck-boost power converter for power transfer. The maximum power point tracking function is achieved through proper control of the power switches of the power converter. A fuzzy logic controller is then developed to perform the MPPT function for obtaining maximum power from the PV panel. The MATLAB based Simulink piecewise linear electric circuit simulation tool is used to verify the complete circuit simulation model.

Keywords: buck-boost converter, PV emulator, maximum power pointing tracking, fuzzy controller

1. Introduction

Solar energy is the most abundant resource on earth. Usages of solar energy are widespread in industry, commercial, and military applications. It will become one of the primary energy supply resources in the future [1, 2]. Effectiveness of the utilization of the solar energy depends on the technologies of the solar power management system. Power converter for maximal power point tracking (MPPT) and voltage or current regulation is inserted between the solar cell panel and the load to control power flow. It directly affects its efficiency and performance of the solar power management system.

To maximize utilization of available solar power drawn from the solar panel and widen the application of solar energy, design and application of buck-boost converters are investigated in many studies [3-7]. [4, 5] developed buck-boost converters for portable applications. [6] proposed a buck-boost cascaded converter for high power applications, such as fuel cell electric vehicles. An extensive analysis and design of Li-ion battery charging using a four-switch type synchronous buck-boost power converter was presented in [7]. In this study, we conduct a comparative study for photovoltaic (PV) panel emulation using different buck-boost converter topologies through circuit simulation including Zeta, SEPIC (single-ended primary-inductor converter), and four-switch type synchronous buck-boost converters.

MPPT function is usually incorporated in the solar power management system to ensure that maximum available power is received from the solar photovoltaic panel. Recently, fuzzy logic controller has received an increased attention to researchers for converter control and MPPT design [8-13]. A reliable and accurate PV emulation model is necessary for accelerating the development of a MPPT system. The PV emulation model has to provide well regulated output voltage and current according to the characteristics of the PV model. A voltage controlled buck converter based PV emulator design is presented in [14]. Design of current controlled buck converter based PV emulator is reported in [15]. In [16], an 8-bit microcontroller controller two-switch buck-boost converter based PV emulator using piecewise linear approach to represent the PV characteristics is reported. Design of a dual-mode power regulator for PV module emulation system is presented in [17]. To avoid switching noise and voltage ripple, [17] uses a linear regulator for the power source instead of using switching type power converters.

In this study, we focus on circuit simulation for buck-boost converter based MPPT system. A voltage and current controlled dual-mode buck-boost converter based PV emulation system is developed first. In this PV emulation system, three buck-boost converter topologies (Zeta, SEPIC, and four-switch type synchronous converter) are investigated. Circuit simulations using MATLAB based Simulink piecewise linear electric circuit simulation tool (PLECS) are conducted for different load conditions. The results show that the proposed buck-boost converter based PV emulation model will accurately emulate the characteristics of the PV panel. After the success of the design and circuit simulation of the PV emulation system, a SEPIC buck-boost converter based MPPT system is then developed using fuzzy logic to perform the MPPT function. The MPPT system is powered by the buck-boost converter based PV emulation system. Circuit simulations for the complete buck-boost converter based MPPT system are successfully verified in MATLAB/Simulink PLECS environment.

2. PV Model

The widely used single-diode equivalent circuit model to represent the characteristics of PV panel for PV system analysis and simulation is shown in Figure 1. The circuit model represents the PV panel as a current source I_{ph} in parallel with a single diode and a shunt resistor R_P, and a series resistor R_S. The current I_{PV} and voltage V_{PV} from the PV panel is characterized by the following equation.

$$I_{PV} = I_{ph} - I_D - \frac{V_{PV} + R_S I_{PV}}{R_P} \tag{1}$$

$$I_D = I_0 \left[\exp\left(\frac{q(V_{PV} + R_S I_{PV})}{nAKT} \right) - 1 \right] \tag{2}$$

where I_{ph} is the current generated by incident light, I_D is the diode current, I_0 is the reverse saturation current, q is the electron charge (1.602×10^{-19} C), K is the Boltzmann constant (1.38×10^{-23} J/K), T is the cell's operating temperature in Kelvin (K), A is the diode ideality constant, and n number of diode in series to form the single-diode model. The current source I_{ph} mainly depends on the sun light irradiation level and operation temperature of the solar panel.

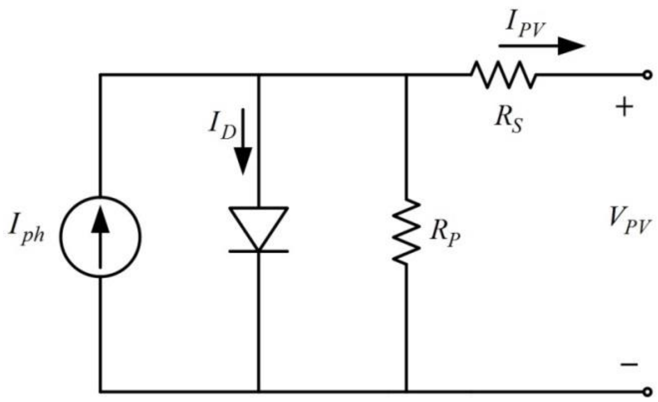

Figure 1. Single-diode equivalent circuit model

In this study, the Solarex MSX60 PV module is chosen to conduct the design and circuit simulation. The key characteristics of the PV panel using parameters listed in [18] are listed in Table 1.

Table 1. Characteristics of the Solarex MSX60 PV panel operate at $20^{\circ}C$.

Irradiation Level, G	1000 W/m^2
Temperature, T	20°C
Open Circuit Voltage	21.5 V
Short Circuit Current	3.788 A
Voltage, Max Power	17.4 V
Current, Max Power	3.55 A
Maximum Power	61.77 W

3. Buck-Boost Converter

The buck-boost converter is capable of converting the supply voltage source to higher and lower voltages to a load terminal. Several commonly used buck-boost converter topologies are shown in Figure 2. The Cuk converter in Figure 2(a) is a inverting type power converter (output voltage polarity is reversed) while the Zeta, SEPIC, and four-switch type topologies in Figure 2(b)-(d) are non-inverting buck-boost converters. The voltage at the load terminal is controlled by continuously adjusting the duty ratio of the power switch of the buck-boost converter. Since voltage polarity at the load end is opposite to that at the source terminal for the Cuk converter, we will only discuss the non-inverting type buck-boost converter topologies (Figure 2(b)-(d)) in this study. Zeta and SEPIC converters contain two inductors, two capacitors, a diode, and a MOSFET power switch. The four-switch type converter in Figure 2(d) is a synchronous buck-boost converter. It contains an inductor, a capacitor, and four MOSFET power switches. The switches Q_1 and Q_3 work as one group and Q_2 and Q_4 work as another group. When Q_1 and Q_3 are turned on, the switches Q_2 and Q_4 will be turn off, and vice versa. In steady state condition, the output voltage of the non-inverting type buck-boost converter is

$$V_O = \frac{D}{1-D} V_S \tag{3}$$

Thus, we can regulate the output voltage to higher or lower than the source voltage through properly control the operating duty ratio for the MOSFET power switches.

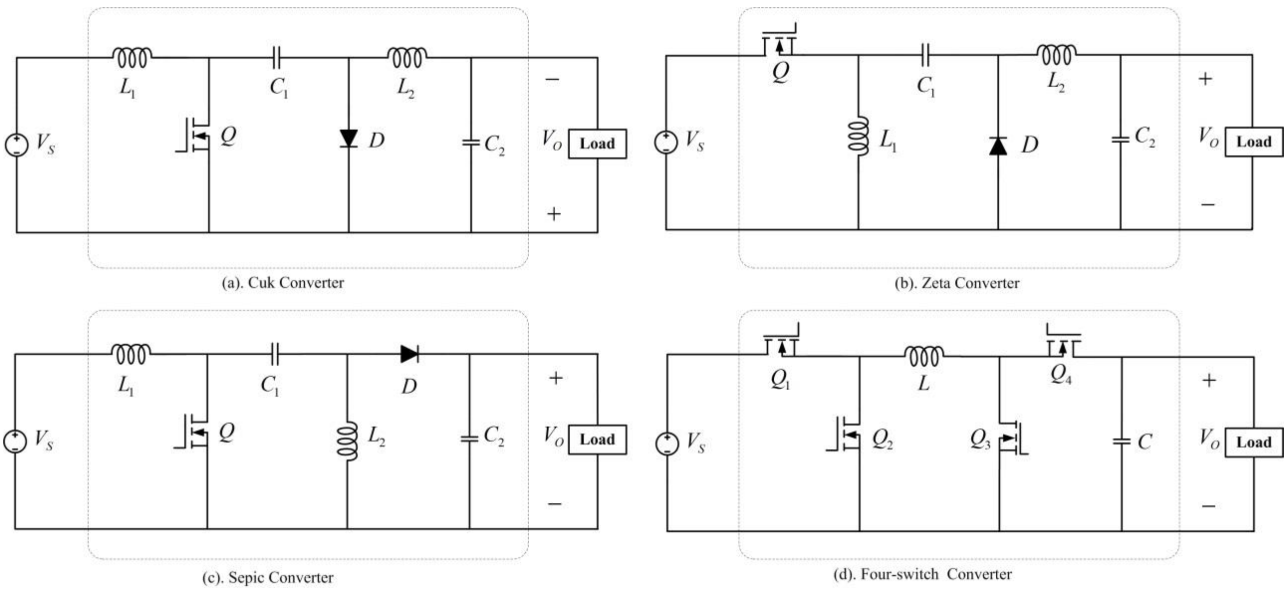

Figure 2. Buck-Boost Converters. (a). Cuk converter, (b). Zeta Converter, (c). SEPIC Converter, (d). Four-switch type converter.

To investigate the performance of the buck-boost converters, circuit simulation for the non-inverting type converters (Figure 2 (b)-(d)) powered by ideal voltage source is conducted in MATLAB/Simulink environment. The characteristic of the buck-boost depends on the value of the inductor and capacitor. The factors which need to be considered for determining the value of the inductance include the input voltage range, the output voltage range, the maximum inductor current, and the switching frequency. The capacitor is used to maintain a well-regulated voltage. The capacitance depends on the inductor current ripple, the switching frequency, and the desired output voltage ripple. For comparison purposes, same parameters are used for all the considered converter topologies. The results for power source $V_S = 20\,\text{V}$, the inductor $L = 150\ \mu\text{H}$, the capacitor $C = 200\ \mu\text{F}$, 3A load, the duty ratio for power switch $D = 0.6$, and 100 kHz switching frequency for the power switches are shown in Figures 3 and 4. Figure 3 indicates the responses during transient period. The desired output voltage is 30V. From the results the four-switch type converter provides faster and smoother transient response than the others. Figure 4 shows the responses in steady-state condition. The averaged steady-state error for the four-switch type converter is about 0.4V, 0.6V for SEPIC converter, and about 0.58V for Zeta converter. The output voltage ripple for the four-switch type converter is about 35 mV, 60 mV for the SEPIC converter, and that for Zeta converter is only about 5 mV. The performance and impact on the design of PV emulator and MPPT system utilizing different he discussed buck-boost converter topologies will be explored further in the following sections.

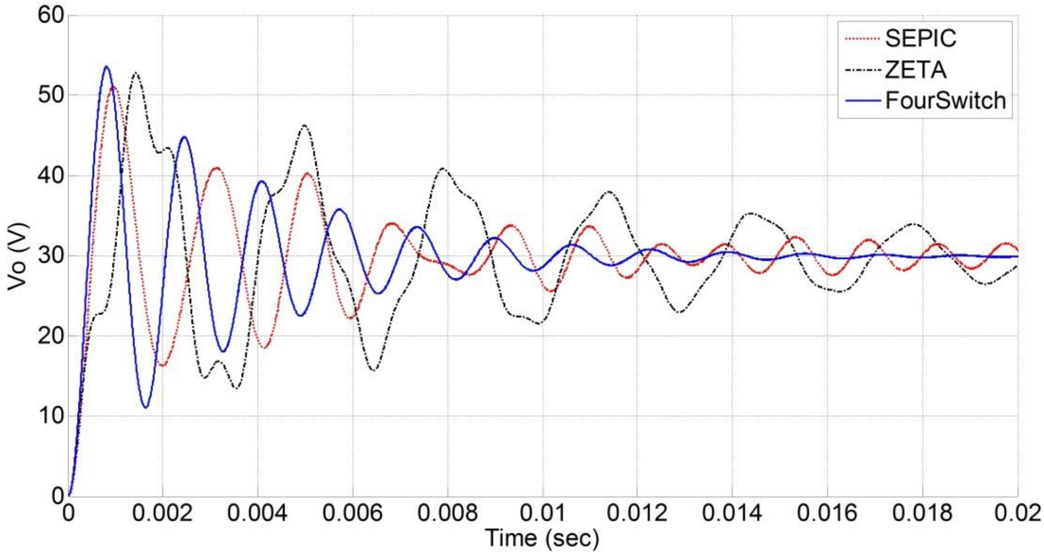

Figure 3. Comparison for transient responses

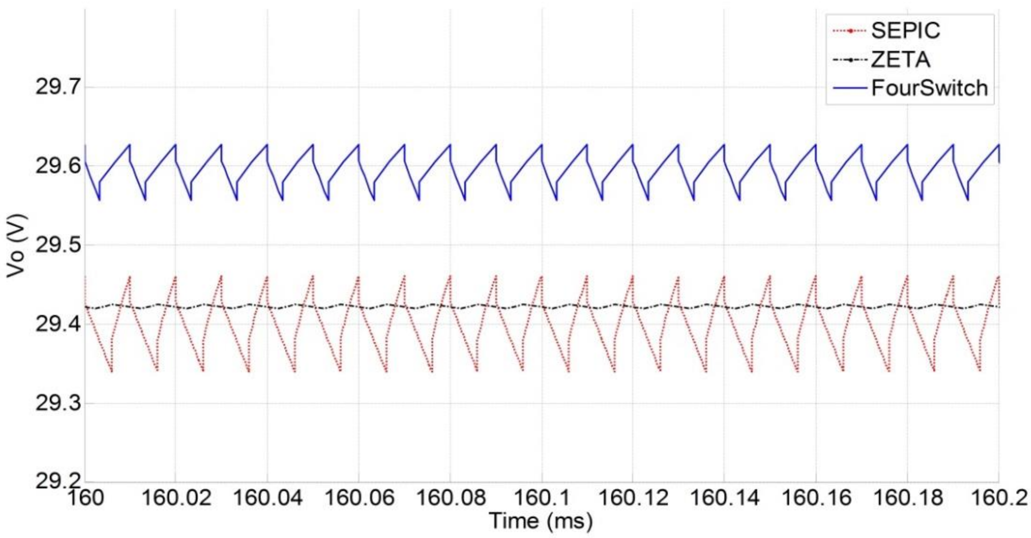

Figure 4. Comparison for steady-state responses

4. PV Emulation Model

A reliable and accurate PV emulation model is necessary for accelerating the development of a MPPT system. The PV emulation model has to provide well regulated output voltage and current according to the characteristics of the PV model shown in Figure 6. A buck-boost converter based dual-mode power regulation system is adopted in this study. Figure 6 depicts the structure of the proposed PV emulation model. The model contains buck-boost converter based voltage regulator and current regulator. Based on the output current the PV model generates a reference output voltage according to the I-V characteristics of the PV model for the voltage regulator to maintain the output voltage to conform to the I-V curve of the PV model. Similarly, the current regulator controls the output current to fit the I-V characteristics of the PV model. The outputs of the voltage regulator and current regulator are connected using ORing diodes as indicated in Figure 6. The regulator with higher output voltage supplies the current to the load. The Mode Control function in Figure 6 monitors the PV panel output voltage V_{PV} , current I_{PV} , voltage regulator output voltage V_{VR} , and current regulator output current I_{CR} to generate the mode control commands (VR and CR) using the voltage regulation threshold voltage V_{VRT} and current regulation threshold current I_{CRT} . The mode transitions and conditions for the mode control proposed in [17] are adapted and implemented using MATLAB functions.

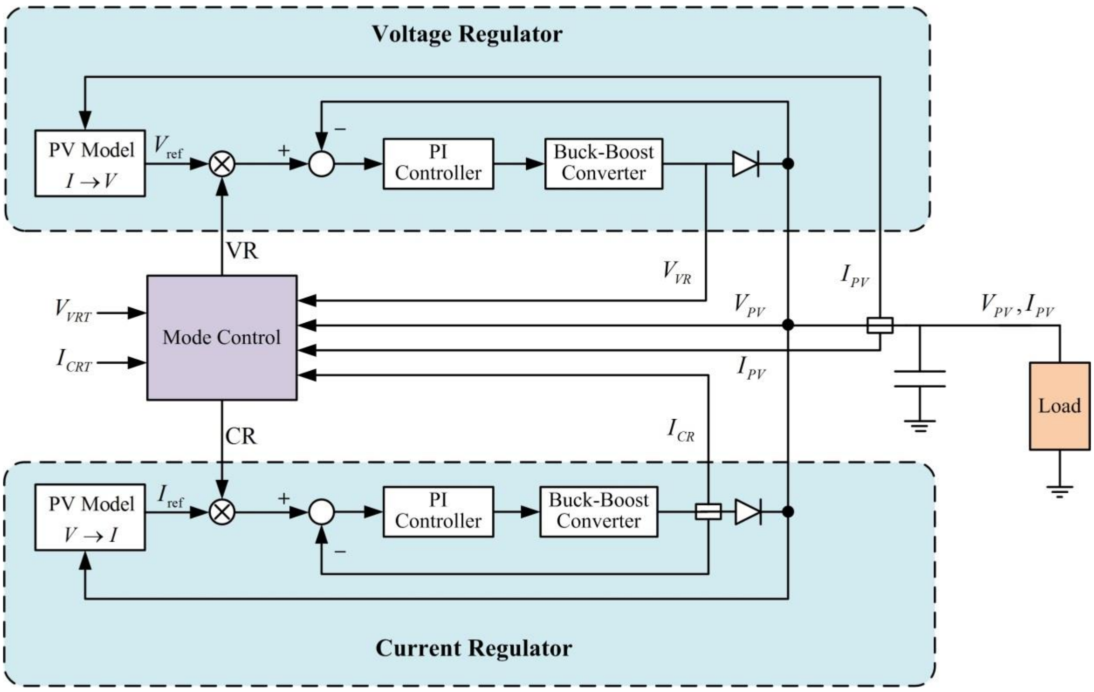

Figure 6. Block diagram of the dual-mode PV emulation system

To verify the performance of the buck-boost converter based PV emulation system, a PLECS based circuit simulation is developed. The block diagram of the circuit simulation model is shown in Figure 7(a). The circuit simulation model contains a PLECS circuit, a MATLAB function based PV model and mode control function. Details of the PLECS circuit are depicted in Figure 8. In this circuit simulation a resistive load is connected to the PV emulator. The I-V characteristics of the PV panel and its corresponding operating points with different resistive loads are shown in Figure 7(b). As indicated in Figure 7(b), the intersection of the I-V characteristic curve of the PV panel and the resistor I-V curve is the operating point of the system. The operating point will be varied if the load resistance R_L is varied. Different converter topologies (Zeta, SEPIC, and four-switch type) based PV emulator with different resistor loads ($3\,\Omega$, $4.9\,\Omega$, and $8\,\Omega$) are tested to investigate the performance of the PV emulator. The $4.9\,\Omega$ load corresponds to the optimal load condition (in sense of maximum power delivered from the PV panel) under this test condition (at $20^{\circ}\mathrm{C}$ with $1000\,\mathrm{W/m^2}$ irradiation level). The voltage and current outputs from PV emulator for different buck-boost converter topologies loaded with different resistive load are presented in Figures 9-11. These results indicate that the PV emulator using all of the three converters nicely performs the I-V characteristics of the PV model when steady state conditions are reached. The results are summarized in Table 2. The results almost perfectly match the I-V characteristics and its corresponding operating points for different load conditions are indicated in Figure 7(b). If we zoom in the results in Figures 9-11 further in a tiny period we will encounter about 0.1% to 0.2% high frequency ripples occur similar to the results in Figure 4 for SEPIC and four-switch type converters. This suggests that Zeta topology could be a better choice for this particular application.

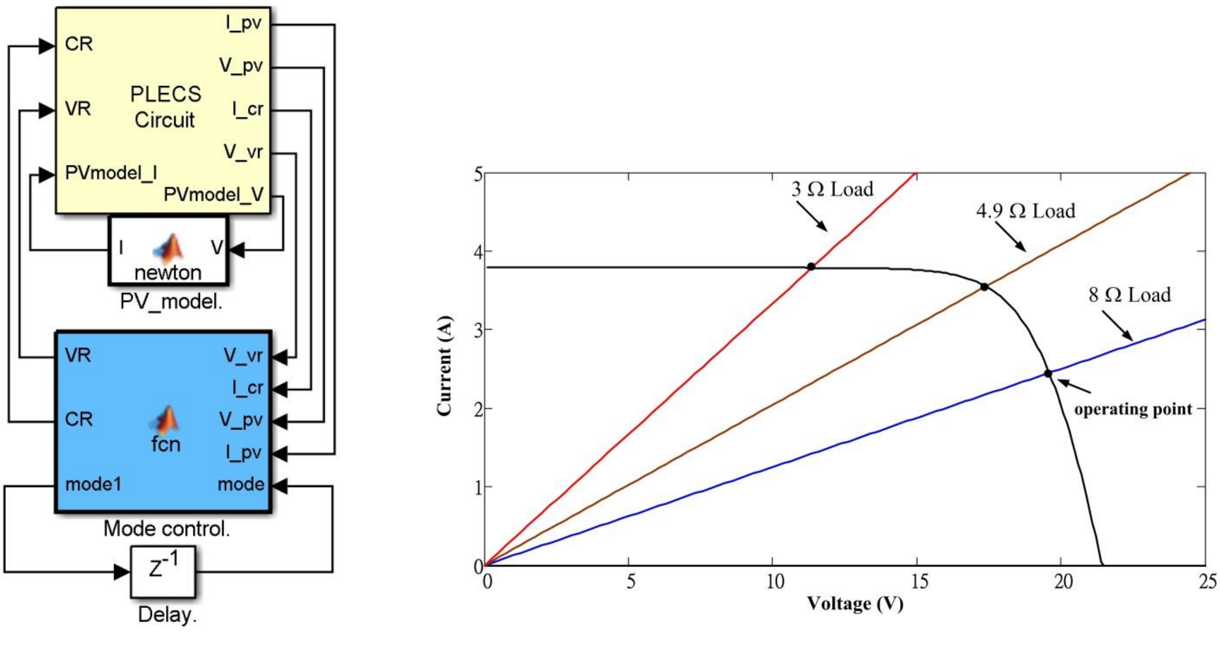

(a)

(b)

Figure 7. (a). Block diagram of the circuit simulation for the buck-boost converter based PV emulation system. (b). I-V characteristics of the PV panel and its corresponding operating points with different resistive loads.

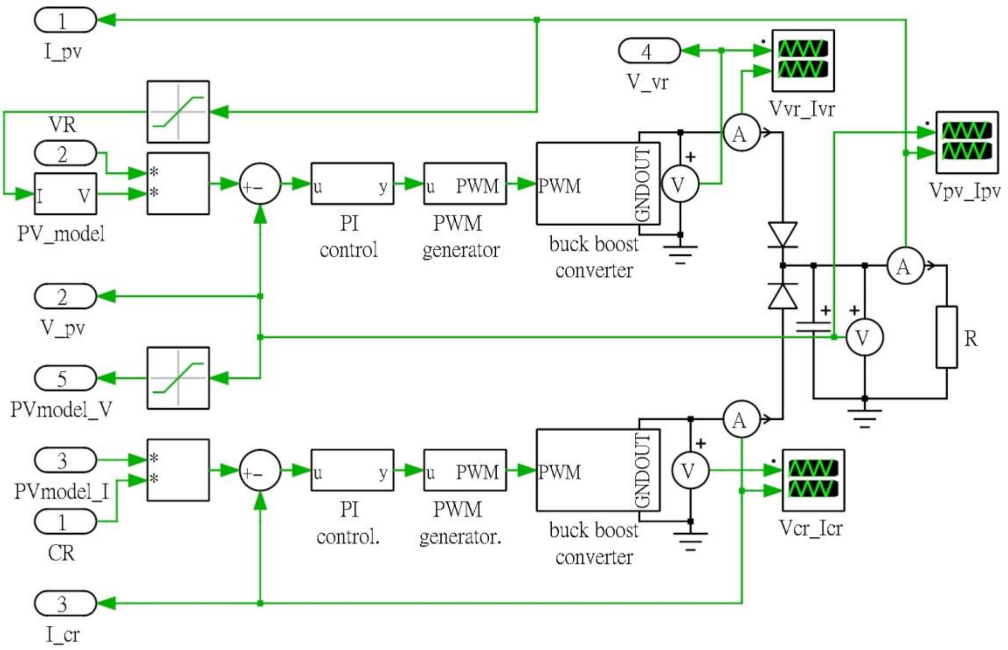

Figure 8. PLECS circuit simulation model for PV emulation with resistive load

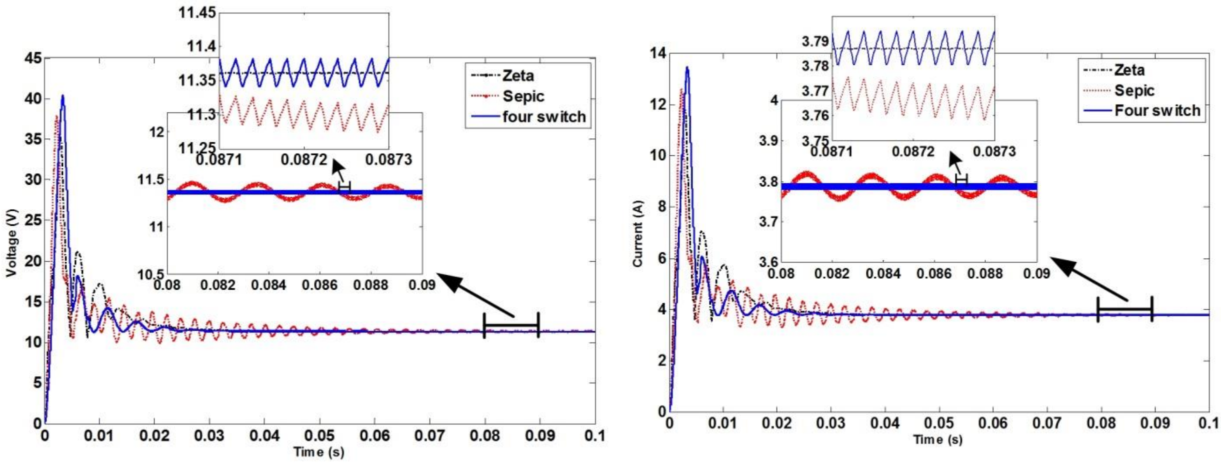

Figure 9. Voltage and current outputs from PV emulator for different buck-boost converter topologies loaded with 3 Ω resistor.

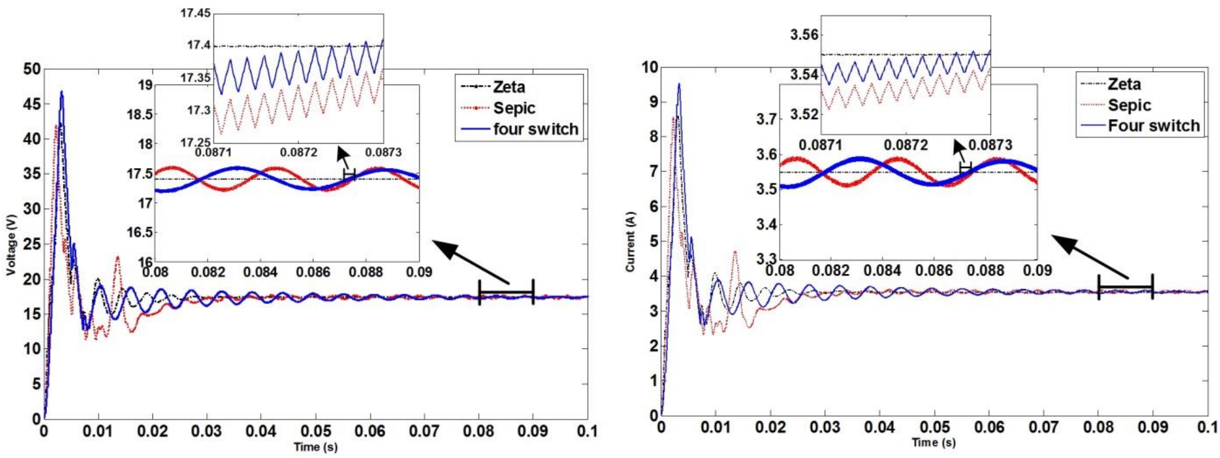

Figure 10. Voltage and current outputs from PV emulator for different buck-boost converter topologies loaded with 4.9 Ω resistor.

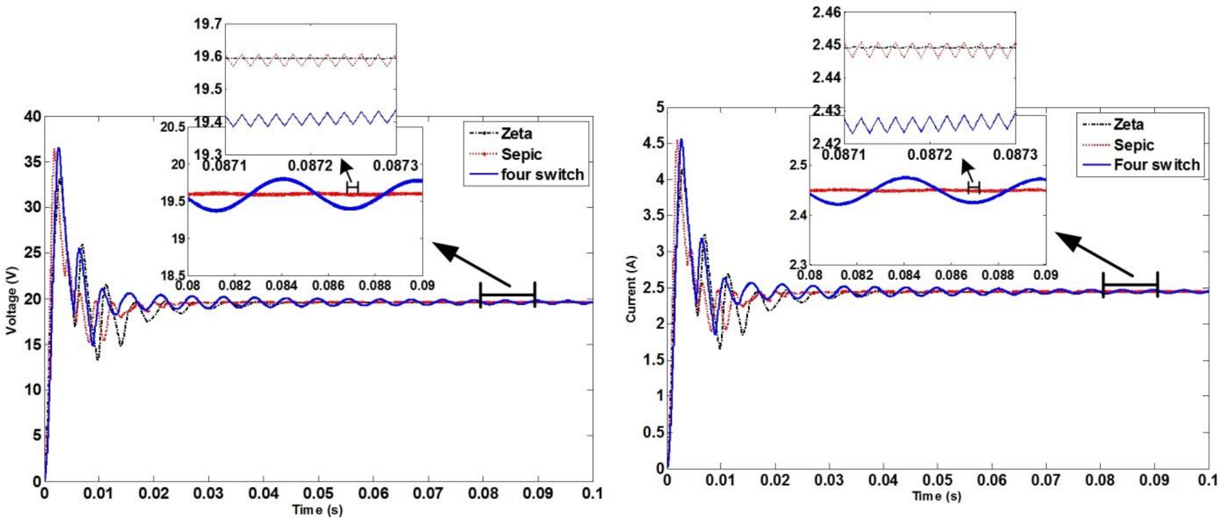

Figure 11. Voltage and current outputs from PV emulator for different buck-boost converter topologies loaded with 8 Ω resistor.

Table 2. Results of PV emulation with different resistive load

Converter Topology	Zeta			SEPIC			Four-Switch Type		
Load	3 Ω	4.9 Ω	8 Ω	3 Ω	4.9 Ω	8 Ω	3 Ω	4.9 Ω	8 Ω
V_{PV} (V)	11.361	17.4	19.597	11.36	17.4	19.595	11.36	17.4	19.6
I_{PV} (A)	3.787	3.55	2.450	3.787	3.55	2.450	3.787	3.55	2.45
P_{PV} (W)	43.024	61.77	48.007	43.020	61.77	47.999	43.020	61.77	48.02
Settling Time (ms)	28.3	22.0	36.8	65.0	36.0	22.0	26.9	63.5	52.6

5. Buck-Boost Converter Based MPPT System

From the results shown in Table 2 the operating point of the PV panel varies if the load resistance varies. Maximum power point may be achieved through proper selection of the load. In most of the cases, the load is not likely to be optimal (in sense of maximum power delivered from the PV panel). Maximum power from the PV panel may be attained by incorporation of some intelligent mechanism to alter the load resistance seen from the PV panel. Power converters are the ones that are widely used to adjust the operating condition to reach the maximum power point.

Figure 12 is the incorporation of a buck-boost converter into a PV system. The load voltage is controlled via proper adjustments of the duty ratio of the power switches of the converter. Assuming the buck-boost converter is operating in continuous conducting mode with 100% efficiency, the relationship of the voltage and current at the load terminal and those at the PV panel at steady-state are

$$V_o = \frac{D}{1-D} V_{PV} \;;\; I_o = \frac{1-D}{D} I_{PV} \tag{3}$$

From Ohm's law, the load resistance can be expressed as

$$R_L = \frac{V_o}{I_o} = \left(\frac{D}{1-D}\right)^2 \frac{V_{PV}}{I_{PV}} \tag{4}$$

Thus, the equivalent resistance seen from the PV panel, denoted as R_{PV}, is

$$R_{PV} = \frac{V_{PV}}{I_{PV}} = \left(\frac{1-D}{D}\right)^2 R_L \tag{5}$$

Equation (5) implies that for a certain load resistance R_L the equivalent resistance R_{PV} only depends on the duty ratio of the buck-boost converter. Hence, we may adjust the duty ratio D to achieve maximum power transfer from the PV panel through some clever mechanism. Figure 13 shows the power characteristics of the PV system and power received at the load terminal with different duty ratio for the power switches of the converter. The power developed at the load terminal is

$$P_L = \frac{V_o^2}{R_L} = \frac{\left(\frac{D}{1-D} V_{PV}\right)^2}{R_L} = \left(\frac{D}{1-D}\right)^2 \frac{V_{PV}^2}{R_L} = \frac{V_{PV}^2}{R_{PV}} \tag{6}$$

The intersection of the PV power curve (blue) and the power curve for the load (red) is the operating point of the PV system. It is clear that maximum power point may be achieved by proper choice of the duty ratio for the power converter. In this study, a fuzzy logic controller is designed to perform the MPPT function.

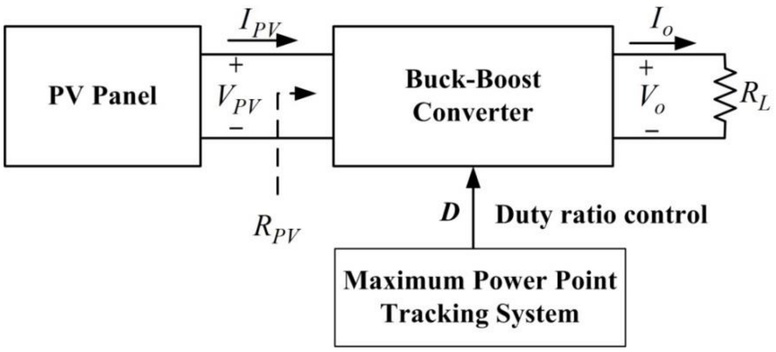

Figure 12. PV system with buck-boost converter incorporated.

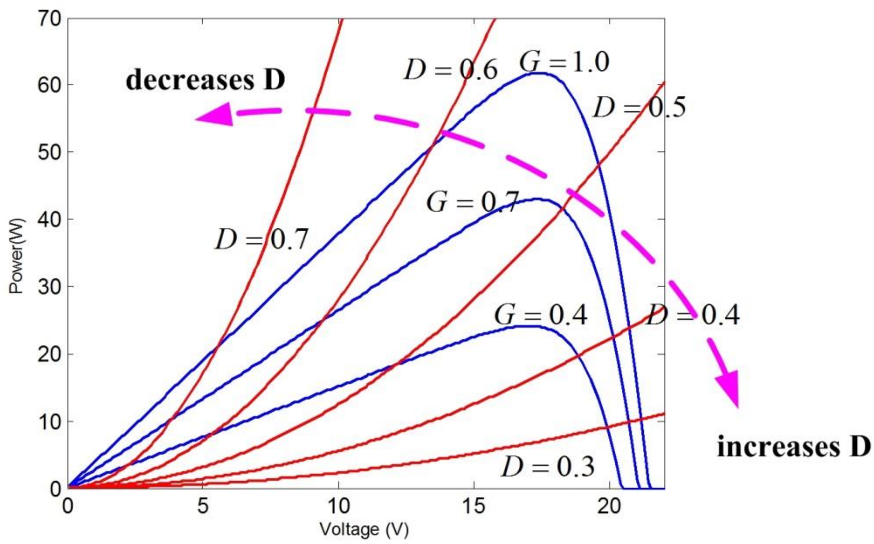

Figure 13. Power characteristics of the PV system.

6. Fuzzy Logic MPPT Controller

The fuzzy logic control system is depicted in Figure 14. The input variables of the fuzzy logic controller are the slope of the power variation $E(n)$ and the change of the slope $\Delta E(n)$ defined as

$$E(n) = \frac{P(n) - P(n-1)}{V_{PV}(n) - V_{PV}(n-1)} \tag{7}$$

$$\Delta E(n) = E(n) - E(n-1) \tag{8}$$

The output variable of the fuzzy logic is the increment ΔD of the duty-ratio command for the power switches. Based on the characteristics of the PV model and features of the buck-boost converter as given in Figure 13, a five-term fuzzy set, Negative Big (NB), Negative Small (NS), Zero (ZE), Positive Small (PS), and Positive Big (PB) is defined to describe each linguistic variable. The fuzzy rules for this MPPT design are shown in Table 3. Figure 15 describes the membership functions for the input and output variables. The fuzzy method used in this buck-boost converter based circuit simulation is Mamdani, in which the maximum of minimum composition technique is used for the inference and center-of-gravity is used for the defuzzification process.

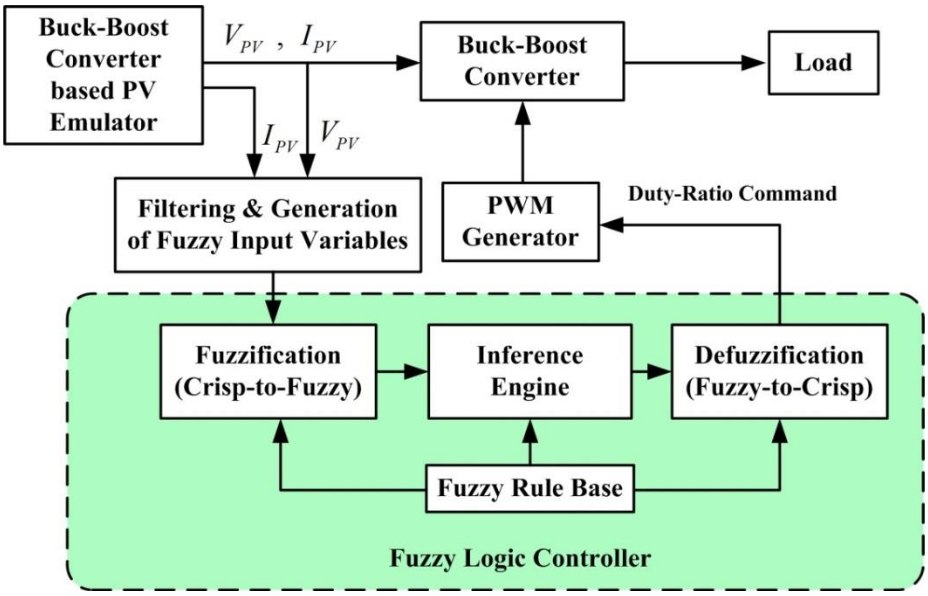

Figure 14. Fuzzy logic controller for the MPPT design.

Table 3. Fuzzy rule table

		$E(n)$				
		NB	**NS**	**ZE**	**PS**	**PB**
$\Delta E(n)$	**NB**	**ZE**	**PS**	**PS**	**ZE**	**NS**
	NS	**PB**	**PS**	**ZE**	**ZE**	**NS**
	ZE	**PB**	**PS**	**ZE**	**NS**	**NB**
	PS	**PS**	**ZE**	**ZE**	**NS**	**NB**
	PB	**PS**	**ZE**	**NS**	**NS**	**ZE**

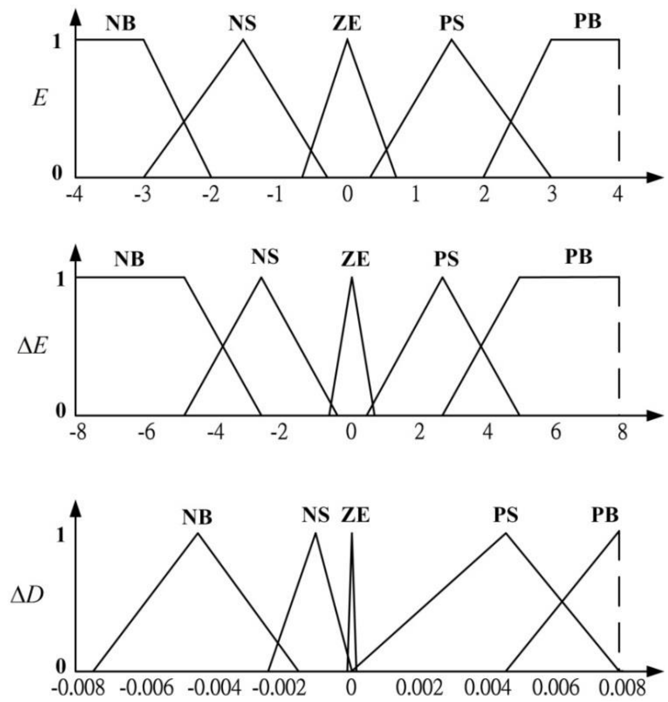

Figure 15. Membership functions for the input and output variables.

The buck-boost converter used for MPPT function is the SEPIC converter. The Zeta and four-switch type converter are not considered suitable for MPPT application due to series switching of the input current which causes loss of input power. Circuit simulation model for the MPPT system and its PLECS circuit are illustrated in Figure 16. Two buck-boost converters are involved in this circuit simulation. One is for the PV emulator and another is for the MPPT function. As discussed in the PV emulator design, three converters can be chosen for the PV emulation model. Similar to the simulation for PV emulation, three different resistive loads (3Ω, 4.9Ω, and 8Ω) are used to evaluate the performance of the fuzzy controller.

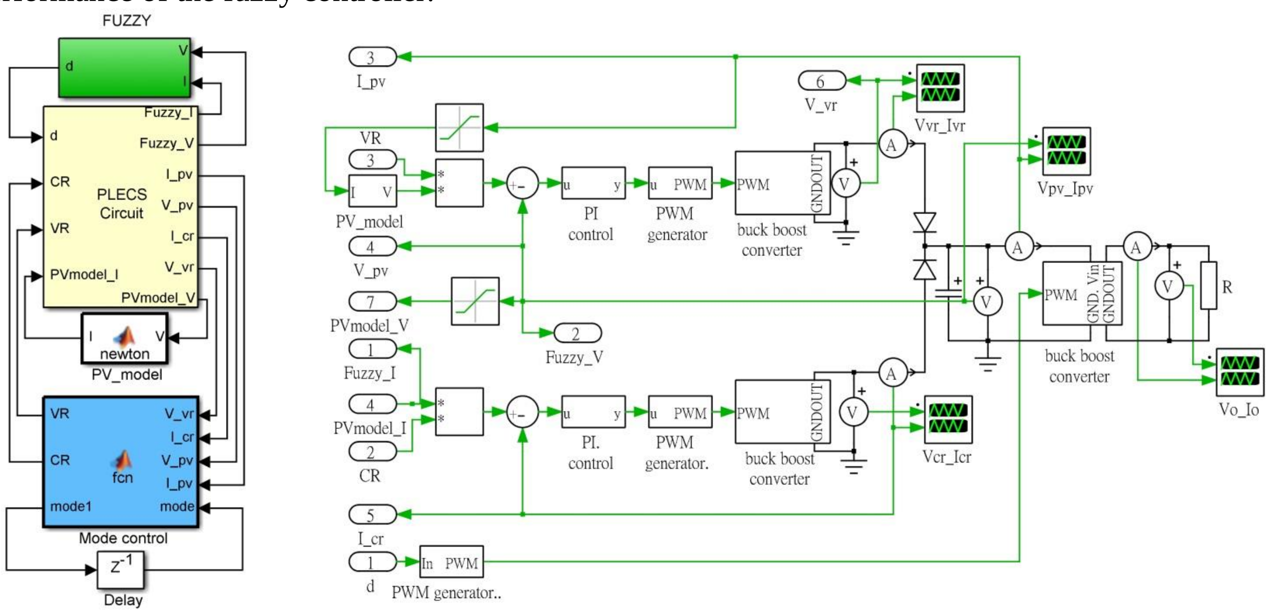

Figure 16. Circuit simulation model for buck-boost converter based MPPT system with its PLECS circuit.

7. Results and Discussions

The voltage and current outputs from the Zeta buck-boost converter based PV emulator for SEPIC buck-boost converter MPPT system loaded with different resistive load are presented in Figures 17-19. Figure 17 shows the results for 3 Ω resistive load. Figure 17(a) represents the power characteristics of the PV panel and power curve for different duty ratio. Analytical value of the duty ratio for maximum power point is 0.44 for $3\,\Omega$ load resistor. The voltage and current from the PV emulator are 17.4V and 3.55A respectively. The steady state duty ratio from the fuzzy controller is 0.4453 (Figure 17 (b)). The results perfectly match the maximum power point as expected. Results for $4.9\,\Omega$ and $8\,\Omega$ loads are shown in Figures 18-19. Again, maximum power points are obtained. Similar results are achieved for Zeta and SEPIC topologies for the PV emulator. The results for the MPPT circuit simulations are summarized in Table 3. As illustrated in Table 3, maximum power points are reached almost perfectly for any combination of the power converters and loads discussed in this study.

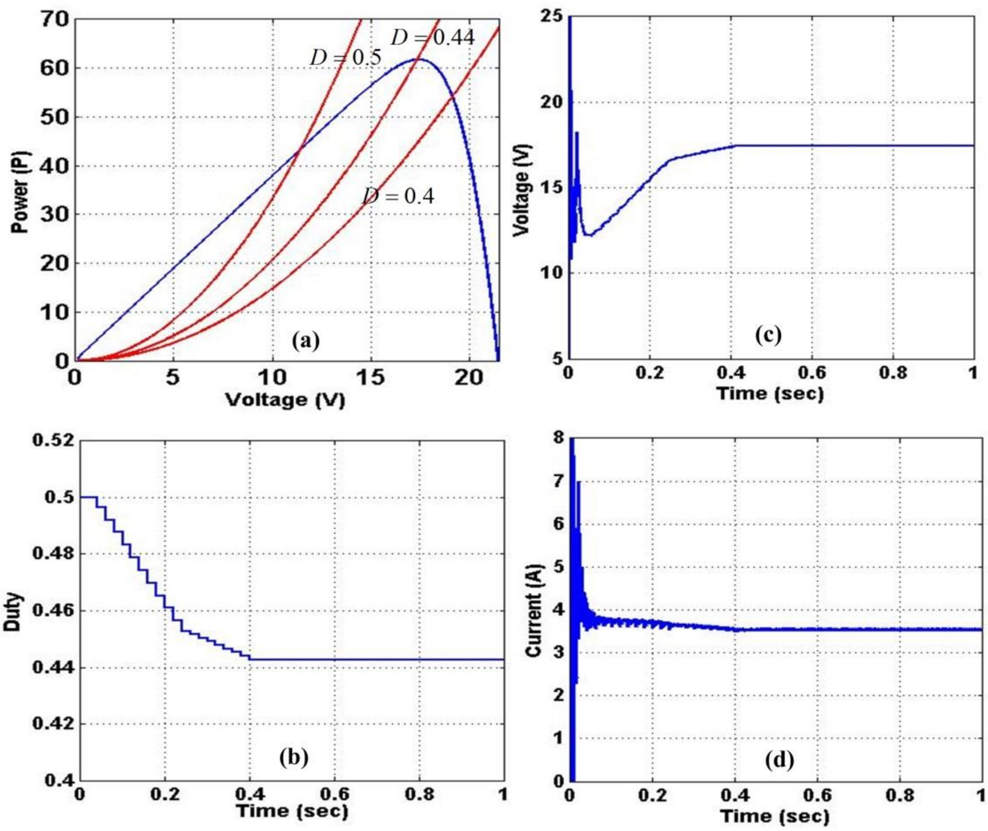

Figure 17. Circuit simulation results with $3\,\Omega$ load. (a). Power characteristics. (b). Duty ratio command. (c). Output voltage from PV emulator. (d). Output current from PV emulator.

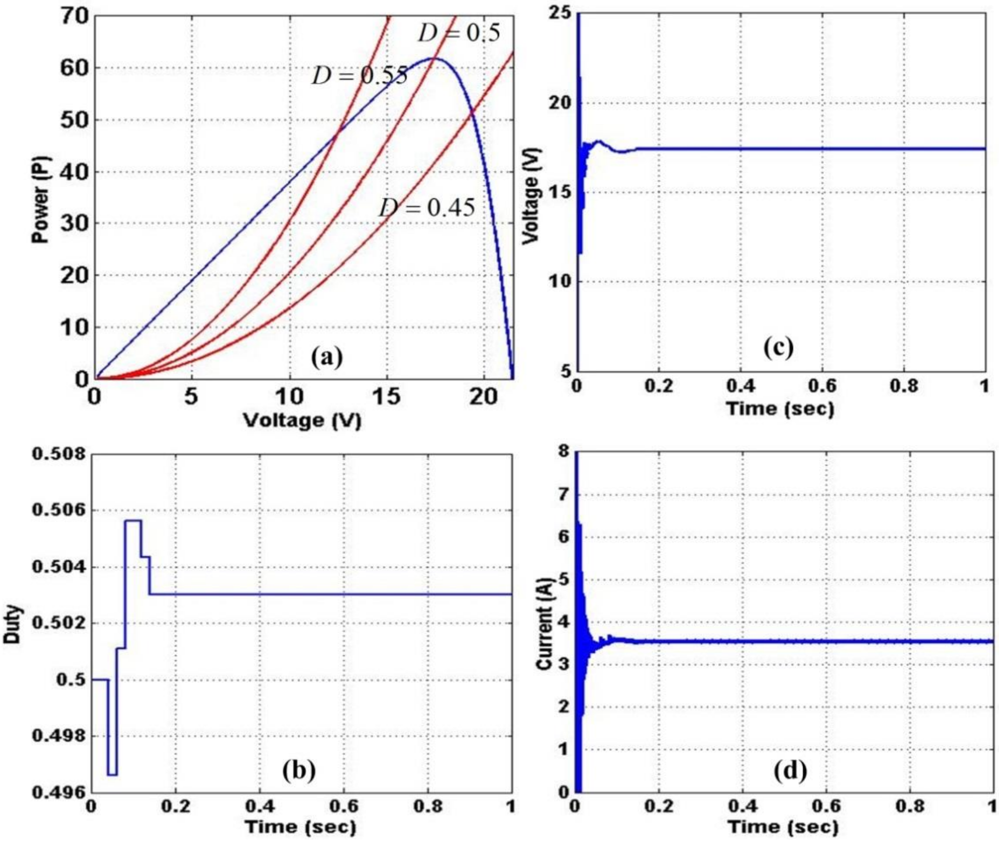

Figure 18. Circuit simulation results with 4.9 Ω load. (a). Power characteristics. (b). Duty ratio command. (c). Output voltage from PV emulator. (d). Output current from PV emulator.

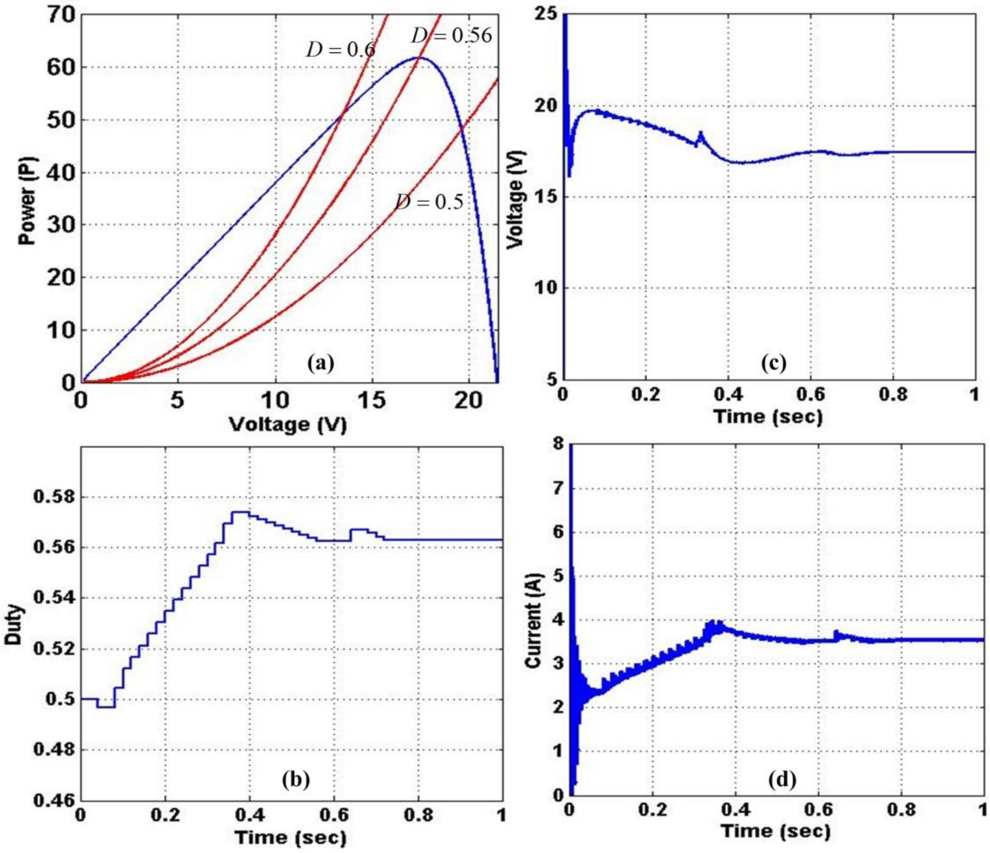

Figure 19. Circuit simulation results with 8 Ω load. (a). Power characteristics. (b). Duty ratio command. (c). Output voltage from PV emulator. (d). Output current from PV emulator.

Table 3. Summaries of the MPPT circuit simulations results

Converter Combination	Zeta -- SEPIC			SEPIC -- SEPIC			Four-Switch -- SEPIC		
Load	3 Ω	4.9 Ω	8 Ω	3 Ω	4.9 Ω	8 Ω	3 Ω	4.9 Ω	8 Ω
V_{PV} (V)	17.448	17.434	17.450	17.44	17.43	17.38	17.40	17.435	17.42
I_{PV} (A)	3.54	3.54	3.530	3.54	3.54	3.55	3.55	3.54	3.542
P_{PV} (W)	61.765	61.71	61.598	61.738	61.702	61.699	61.77	61.72	61.702
Duty Ratio	0.4428	0.5030	0.5631	0.4428	0.5030	0.5639	0.4435	0.5030	0.5634

8. Conclusion

This paper presents the development of a circuit simulation model for solar power maximum power point tracking (MPPT) evaluation with different buck-boost converter topologies including SEPIC, ZETA, and four-switch type buck-boost DC/DC converters. The circuit simulation model includes a PV emulator model, a buck-boost converter based MPPT system, and a fuzzy logic MPPT controller. A voltage and current controlled dual-mode buck-boost converter based PV emulation model is built to emulate the characteristics of the PV panel. The PV emulator is useful for MPPT system design. From this study, all of the three buck-boost converters can successfully provide power regulation to emulate the I-V characteristics of a PV panel. Among them, the Zeta topology contains the least high frequency ripples. The SEPIC topology is used for the MPPT system. Circuit simulations for the complete buck-boost converter based MPPT system are successfully verified in MATLAB/Simulink PLECS environment. The results show that maximum power points are reached almost perfectly for different load conditions.

Acknowledgement

This research was supported by the National Science Council, Taiwan, Republic of China, by grant NSC102-2221-E-032-017.

References

1. International Energy Agency. *Technology Roadmap: Solar Photovoltaic Energy*; IEA Publications: Paris, France, 2010. Available online: http://www.iea.org/publications/freepublications/publication/pv_roadmap-1.pdf . (accessed on 19 February 2014).
2. Ken Tomabechi, "Energy Resources in the Future", *Energies,* 2010, Vol.3, pp.686-695.

3. Weissbach, R. S., and Torres, K. M., “A Non-inverting Buck-Boost Converter with Reduced Components Using a Microcontroller”. *Proceedings of the Southeast Conference 2001,* South Carolina, 30 March-1 April, 2001, pp.79-84.
4. Sahu B., and Rincon-Mora, G.A, “A Low Voltage, Dynamic, Noninverting, Synchronous Buck-Boost Converter for Portable Application”, *IEEE Transactions on Power Electronics*, 2004, Vol. 19, No.2,: pp. 443-452.
5. Gaboriault, M., and Notman, A., “A High Efficiency, Non-Inverting, Buck-Boost DC-DC Converter”, *Applied Power Electronics Conference and Exposition, 2004. APEC’04. Niniteenth Annual IEEE* ,vol.3 ,pp. 1411-1415.
6. Qiao, H., Zhang, Y., Yao, Y., and Wei, L., “Analysis of Buck-Boost Converter for Fuel Cell Electric Vehicles”. *IEEE International Conference on Vehicular Electronics and Safety, 13-15 DEC. 2006,* pp.109-113.
7. Shiau, J.-K. and Ma, C.-W, “Li-Ion Battery Charging with a Buck-Boost Power Converter for a Solar Powered Battery Management System”, *Energies*, 2013, Vol. 6, pp.1669-1699.
8. T. Wu, T., Chang, C., and Chen, Y., “A Fuzzy-Logic-Controlled Single-Stage Converter for PV-Powered Lighting System Applications” *IEEE Trans. Industrial Electronics,* vol. 47, no. 2, pp. 287-296, April 2000.
9. Alajmi, B. N., Ahmed, K. H., Finney, S. J., and Williams, B. W., “Fuzzy-Logic-Control Approach of a Modified Hill-Climbing Method for Maximum Power Point in Microgrid Standalone Photovoltaic System”, *IEEE Trans. Power Electronics,* vol. 26 no. 4, pp. 1022-1030, April 2011.
10. Pongsakor Takun, Somyot Kaitwanidvilai and Chaiyan Jettanasen, “Maximum Power Point Tracking using Fuzzy Logic Control for Photovoltaic Systems” Proceedings of the International MutiConference of Engineers and Computer Scientists, 2011, Vol II, IMECS 2011, March 16-18, Hong Kong.
11. Khateb, A. E., Rahim, N. A., Selvaraj, J., and Uddin, M. N., “Fuzzy Logic Controller Based SEPIC Converter of Maximum Power Point Tracking”, IEEE Industry Application Society Annual Meeting (IAS) 2012, Oct-10-11, Las Vegas, NV, U.S.A., pp.1-9.
12. Liu, C.-L, Chiu, Y.-S, Liu, Y.-H, Ho, Y.-H, and Huang, S.-S, “Optimization of a Fuzzy-Logic-Control-Based Five-Stage Battery Charger Using a Fuzzy-Based Taguchi Method”, *Energies*, 2013, Vol.6, pp. 3528-3547.
13. Venkatanarayanan, S. and Saravanan, M., “Fuzzy Logic Based PV Energy System with SEPIC Converter”, *Journal of Theoretical and Applied Information Technology*, 2014, Vol. 59, No. 1, pp. 89-95.
14. CAN, H., “Model of a photovoltaic panel emulator in MATLAB-Simulink”, *Turkish Journal of Electrical Engineering & Computer Sciences*, vol. 21, pp. 301,308, 2013.
15. Rana, A. V. and Patel, H. H., “Current Controlled Buck Converter based Photovoltaic Emulator”, *Journal of Industrial and Intelligent Information*, Vol. 1, No. 2, June 2013, pp. 91-96.
16. Lu, D. D. C., and Nguyen, Q. N., “A photovoltaic panel emulator using a buck-boost DC/DC converter and a low cost micro-controller” *Solar Energy*, 2012, Vol. 86, pp. 1477-1484.
17. Kim, Y., Lee, W., Pedram, M., and Chang, N., “Dual-mode power regulator for photovoltaic module emulation”, *Applied Energy*, Vol. 101, pp. 730-739, 2013.

18. Walker G., “Evaluating MPPT Converter Topologies Using A MATLAB PV Model”, Journal of Electrical & Electronics Engineering, Vol. 21, 2001, pp. 49-55.